CMS Physics Analysis Summary

Contact: cms-pag-conveners-susy@cern.ch 2011/04/14

Search for Supersymmetry in Final States with b Jets and Missing Energy at the LHC

The CMS Collaboration

Abstract

A search for supersymmetry in final states with b jets and large transverse momentum imbalance is presented. The search is carried out in a data sample collected with the CMS detector of proton-proton collisions delivered by the LHC at a centre-of-mass energy of 7 TeV, corresponding to an integrated luminosity of 35 pb^{-1}. A total of $0.33^{+0.43}_{-0.33}$ (stat) $\pm$ 0.13 (syst) events is predicted directly from data to arise from standard model processes, and one event is observed in the data. Upper limits are set at the 95% confidence level on the cross sections of benchmark supersymmetry models.

1 Introduction

Supersymmetry (SUSY) [1–5] is an extension to the standard model (SM) of particle physics, which can solve the "hierarchy problem" [6, 7] and provide a cold dark matter candidate [8]. For a large class of supersymmetric parameter sets, squarks ($\tilde{q}$), the SUSY partners of quarks (q), are relatively light. In this case, significant event yields at the Large Hadron Collider (LHC) can result from strong production of squarks, which decay to the weakly interacting lightest supersymmetric particle, or LSP. If sbottoms ($\tilde{b}$) and stops ($\tilde{t}$), which can decay to b quarks, are relatively light, there may be an abundance of events with momentum imbalance transverse to the beam line due to the LSP [9] and one or more b quark jets.

This document describes a search for events with two or more hadronic jets in the final state, significant transverse momentum imbalance, and a b-tagged jet [10], and extends a similar search without a b-tag requirement [11]. The momentum imbalance is characterized by the variable α_T, which is defined in Section 3.

The main backgrounds are due to standard model multi-jet production (hereafter denoted "QCD background"), electroweak W and Z boson production (EWK), and top quark pair production ($t\bar{t}$). The QCD background is effectively rejected, due to low average $\not{H}_T$, by a requirement on α_T, and the b-tag requirement further suppresses the QCD and EWK backgrounds.

The results of the search are characterized in terms of a class of SUSY models known as the Constrained Minimal Supersymmetric extension of the Standard Model (CMSSM) [12]. These models are described by four parameters and one sign: the universal scalar and gaugino mass parameters, m_0 and $m_{1/2}$, respectively; the universal trilinear coupling, A_0; the ratio of the two Higgs doublet vacuum expectation values, $\tan\beta$; and the sign of the Higgs mixing parameter, sign(μ). Three signal benchmark points are considered: LM0, LM1, both discussed in Ref. [11], and LMB (corresponding to $m_0 = 400$ GeV, $m_{1/2} = 200$ GeV, $A_0 = 0$ GeV, $\tan\beta = 50$, and sign$(\mu) > 0$), chosen to be near the edge of sensitivity of this search in CMSSM space.

The organization of this document is as follows: A brief description of the CMS detector is given in Section 2 and the α_T variable is discussed in Section 3. Section 4 describes the details of event selection. Section 5 discusses the relevant backgrounds and their estimation. The signal efficiency and acceptance are studied in Section 6, with corresponding systematic uncertainties described in Section 7. Section 8 discusses the results of the search and Section 9 concludes.

2 The CMS Detector

The analysis presented here utilizes 35 pb^{-1} of data collected by the CMS detector from proton-proton collisions delivered by the LHC at a centre-of-mass energy of 7 TeV. The CMS detector is a magnetic spectrometer with a 6 m diameter superconducting solenoid which provides a 3.8 T axial magnetic field. Within the field volume are the silicon pixel and strip tracker, the crystal electromagnetic calorimeter (ECAL) and the brass/scintillator hadron calorimeter (HCAL). Muons are measured in gas-ionization detectors embedded in the steel return yoke. A detailed description of the detector and its performance can be found in Ref. [13]. Useful coordinates for the cylindrical geometry of CMS are the azimuthal angle (ϕ) and pseudo-rapidity (η), defined as $\eta = -\ln\tan\theta/2$, where θ is the polar angle with respect to the counterclockwise beam direction.

3 The α_T Variable

As stated previously, α_T characterizes the momentum imbalance of jets in the transverse plane. For a two jet system, it is defined as

$$\alpha_T = \frac{E_T^{j2}}{M_T^{j1,j2}}, \tag{1}$$

where $j2$ is the jet with lower transverse energy ($E_T = E \sin\theta$) and $M_T^{j1,j2}$ is the invariant mass in the transverse plane of the two jets. Assuming massless jets, this can be rewritten for multi-jet events as

$$\alpha_T = \frac{1}{2} \frac{H_T - \Delta H_T}{\sqrt{H_T^2 - \not{H}_T^2}}, \tag{2}$$

where $\not{H}_T = |\sum_i \vec{p}_T^{\,j_i}|$, $H_T = \sum_i p_T^{j_i}$, and $p_T \equiv p \sin\theta$. The jets in an event are grouped into two pseudo-jets and ΔH_T is the minimal value of $|p_T^{\text{pseudojet1}} - p_T^{\text{pseudojet2}}|$ over all combinations. To partition the multi-jet system into two pseudo-jets, the jets are separated into two groups and the momenta of jets in each group are vectorially summed.

α_T is particularly effective at rejecting QCD background events, which would otherwise be the dominant background because of the large QCD cross section. In well measured QCD events, $\not{H}_T$ will be small, resulting in $\alpha_T \leq 0.5$. Due to finite jet energy and phi resolution, an $\alpha_T > 0.55$ requirement is used for the final event selection in this analysis. In SUSY events, there will be real missing transverse momentum due to the production of LSPs. From Eq. 2, when $\not{H}_T$ is a significant fraction of H_T, as would be the case in many SUSY events, α_T can be greater than 0.55.

Despite the fact that $\alpha_T < 0.55$ for well measured QCD background events, this may not be the case in poorly measured QCD events. In the case that a jet in the event is greatly under-measured or multiple jets fall below the jet E_T threshold and are not included in the α_T calculation, the resulting $\not{H}_T$ can be great enough to cause α_T>0.55. Because a SUSY signal would occur at high H_T, understanding how often α_T fails to reject QCD background events as a function of H_T is important for predicting this background.

4 Event Selection

Before an event can be saved and analyzed, it must meet the requirements of at least one trigger during data taking. Events in the search sample are collected with a set of triggers based on the H_T computed from jets reconstructed at trigger level. These triggers are measured to be over 99% efficient for events passing the final search selection. For background estimation purposes, a muon enriched control sample is collected with triggers requiring a muon. Events must also have a good reconstructed pp collision vertex [14].

Jets are reconstructed as clusters of energy in the calorimeter by the anti-k_T algorithm [15] with a distance parameter of 0.5. Jets are required to have $E_T > 50$ GeV and $|\eta| < 3$ as well as pass a set of identification criteria designed to reject calorimetric noise [16]. To protect against poorly measured jets, an event is rejected if it contains a jet that passes the E_T requirement but fails one of the other requirements.

In order to perform an a fully hadronic final state search as well as reduce the background, we veto events with an isolated lepton (electron or muon) or photon. This is particularly important

in rejection of W and $t\bar{t}$ events with leptonic W decays. In these types of events, a neutrino (ν) is produced in the decay and goes undetected, resulting in transverse momentum imbalance.

Photon candidates [17] are required to have $E_T > 25$ GeV and $|\eta| < 2.5$. The ratio of energy deposited in the HCAL to that in the ECAL must be less than 5%.

Electron candidates [18] are required to have $E_T > 10$ GeV and $|\eta| < 2.5$. The ratio of energy deposited in the HCAL to that in the ECAL as well as the shower shape in the η direction must be consistent with that of an electron. The associated track must be closely matched to the calorimeter deposit in both η and ϕ.

Muon candidates [19] are required to have $p_T > 10$ GeV and $|\eta| < 2.5$. The muon candidate must have a well measured track reconstructed in both the tracker and muon sub-detectors. A global fit to these combined measurements should be of reasonable quality. To select promptly produced muons, the track must also pass within 2 mm of the collision point.

To differentiate promptly produced lepton and photon candidates from those from jets, a restriction is placed on the maximum amount of surrounding energy in the calorimeter as well as the sum of the p_T of nearby, in η and ϕ, tracks in the tracker. Leptons and photons passing this requirement are said to be isolated. Events containing an isolated lepton or photon passing the identification criteria are vetoed. Events are also rejected if they contain a photon or lepton candidate passing the E_T (p_T) and η requirements that is not within a $\Delta R \equiv \sqrt{\Delta\eta^2 + \Delta\phi^2} < 0.5$ cone of a jet. In the case that a muon is within a $\Delta R < 0.5$ cone of a jet, the momentum of the muon is added to that of the jet. However, if the p_T of the muon is greater than half of the E_T of the overlapping jet, the event is rejected because the jet is likely poorly measured. Events are also rejected if they contain a muon candidate that passes the p_T and η requirements but fails one of the other requirements besides isolation.

One potential cause of significant jet under-measurement is overlap of a jet with an ECAL region with multiple adjacent inactive readout channels. The ECAL has a small number of such regions which account for less than 1% of the total acceptance. If a jet showers in the vicinity of one of these regions, a significant portion of its electromagnetic energy can go unmeasured, creating $\not{H}_T$. To reject events of this type, the jet most likely to have been mis-measured is identified as the jet whose transverse momentum is closest in ϕ to the $\vec{\not{H}}_T = -\sum_i \vec{p}_T^{\,j_i}$ computed after removing that jet from the event. If the minimum $\Delta\phi$ is less than 0.5 and the corresponding jet is $\Delta R < 0.3$ away from an inactive ECAL region, the event is rejected. Jets with $E_T > 30$ GeV are used in the above calculation in order to increase the effectiveness of the veto.

Another effect that can artificially create $\not{H}_T$ arises when multiple jets in an event fall below the jet E_T threshold and are not taken into account in the $\not{H}_T$ calculation. However, the energy of these jets is expected to be accounted for in the $\not{E}_T$, which vectorially sums all calorimeter energy regardless of jet clustering. To reject events of this type, we require $\not{H}_T / \not{E}_T < 1.25$.

In addition to the above selection, the final selection requirements are: Two jets with $E_T >$ 100 GeV, $|\eta| < 2.5$ for the highest E_T jet, $H_T > 350$ GeV, at least one jet tagged as originating from a b quark, and $\alpha_T > 0.55$.

The discriminator used for b tagging is the impact parameter significance of the track with the third highest significance in the jet (Track Counting High Purity, or TCHP, discriminator [10]). There are three b-tagging working points corresponding to different TCHP requirements, namely, loose for TCHP > 1.19, medium for TCHP > 1.91, and tight for TCHP > 3.41. The tight selection, designed to have a light flavour contamination of 0.1%, is used in the main analysis, while the other selections are used in various control samples. Because the pixel

tracker coverage extends to $|\eta| < 2.4$, only jets with central axis in this region are considered for b tagging.

5 Backgrounds and Their Estimation

The backgrounds for this search can be categorized into three main groups, namely, QCD, EWK, and $\mathrm{t\bar{t}}$. The vast majority of events from the QCD background do not feature large transverse momentum imbalance and are therefore rejected by the $\alpha_\mathrm{T} > 0.55$ requirement. The EWK backgrounds consist of W and Z boson production, with real missing energy carried away by neutrinos. The requirement of at least one b jet greatly reduces the EWK and QCD backgrounds. The dominant background for the analysis comes from $\mathrm{t\bar{t}}$ production, in which b jets and real missing energy due to neutrinos can arise from the top quark decay chains.

A data-driven procedure, described in Section 5.1, is employed to simultaneously estimate all backgrounds. In this method, the fraction of all events with $\alpha_\mathrm{T} > 0.55$, denoted $\mathrm{F}(\alpha_\mathrm{T} > 0.55)$, is measured in a lower H_T control region and applied in the signal region.

The $\mathrm{Z} \to \nu\bar{\nu}$ and $\mathrm{t\bar{t}}$ background yields are cross checked separately in Section 5.2 and Section 5.3, respectively. The $\mathrm{t\bar{t}}$ cross check uses muons to emulate the hadronic decays of taus. The cross check of $\mathrm{Z} \to \nu\bar{\nu}$ utilizes $\mathrm{Z} \to \mu^+\mu^-$ events for which α_T is determined after the excluding the muons.

5.1 Background Prediction Using α_T vs H_T Extrapolation

With fixed jet E_T thresholds, the topological and kinematic properties of events, in particular $\mathrm{F}(\alpha_\mathrm{T} > 0.55)$, can have a strong dependence on H_T. To remove this dependence, jet E_T threshold values that scale with H_T are used. For $H_\mathrm{T} \in [250, 300]$ GeV, the requirements are jet $E_\mathrm{T} >$ 35.7 GeV and two jets with $E_\mathrm{T} > 71.4$ GeV. For $H_\mathrm{T} \in [300, 350]$ GeV, the requirements are jet E_T > 42.9 GeV and two jets with $E_\mathrm{T} > 85.7$ GeV. For $H_\mathrm{T} \in [350, \infty]$ GeV, the requirements are jet $E_\mathrm{T} > 50$ GeV and two jets with $E_\mathrm{T} > 100$ GeV.

As studied extensively in Ref. [11], this threshold scaling causes $\mathrm{F}(\alpha_\mathrm{T} > 0.55)$ to be independent of H_T in samples where significant $\not{H}_\mathrm{T}$ comes predominantly from real sources. In the QCD background, however, $\mathrm{F}(\alpha_\mathrm{T} > 0.55)$ is expected to be a decreasing function of H_T due to the H_T dependence of the factors contributing to artificial $\not{H}_\mathrm{T}$, such as jet energy resolution and jet E_T threshold effects.

Loosening the α_T requirement to 0.51 reduces the amount of $\not{H}_\mathrm{T}$ needed to have α_T above threshold and causes the QCD background to dominate. This is shown in Fig. 1. The two jet and greater than two jet cases are shown separately. The samples are further divided into events with no loose b-tagged jets (anti-tagged), at least one loose tagged jet, and at least one tight tagged jet. It is clear that $\mathrm{F}(\alpha_\mathrm{T} > 0.51)$ is a decreasing function of H_T in the three or more jet case for $H_\mathrm{T} < 350$ GeV. For H_T above this point, $\mathrm{F}(\alpha_\mathrm{T} > 0.51)$ seems to flatten out, indicating that QCD no longer dominates. To more clearly illustrate the fall of $\mathrm{F}(\alpha_\mathrm{T} > 0.51)$ with H_T, this figure has been binned in 20 GeV slices of H_T, where the jet E_T thresholds are scaled in each bin of H_T, rather than the 50 GeV slices described above.

Although the data is used to estimate the background, the procedure is also validated in Monte Carlo (MC) simulation of SM processes. Figure 2 shows $\mathrm{F}(\alpha_\mathrm{T} > 0.55)$ vs H_T in simulation for all SM processes combined. The event samples for all SM processes are generated via MADGRAPH [20]. In all cases, $\mathrm{F}(\alpha_\mathrm{T} > 0.55)$ is consistent with having no H_T dependence.

To enrich the data sample with QCD background events, the $\not{H}_\mathrm{T}/\not{E}_\mathrm{T} < 1.25$ requirement, which

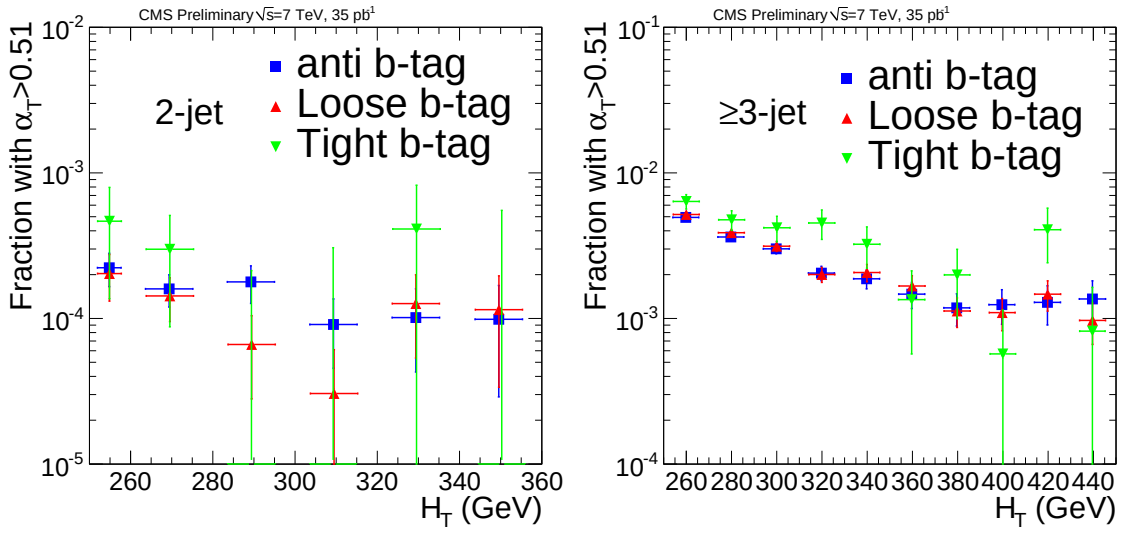

(a) (b)

Figure 1: $F(\alpha_T > 0.51)$ vs H_T in data. $F(\alpha_T > 0.51)$ is a decreasing function of H_T for lower H_T, indicating that QCD dominates these regions.

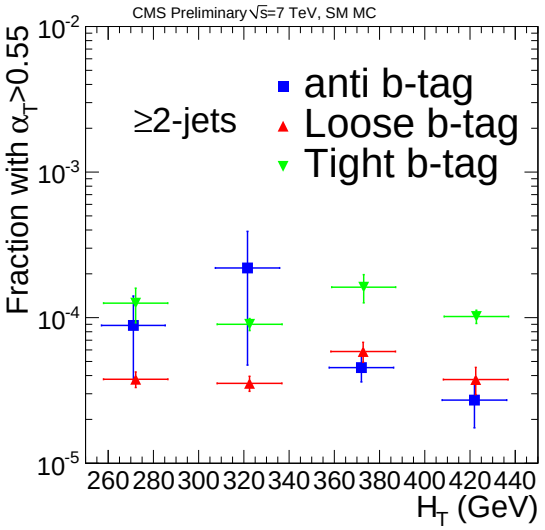

Figure 2: $F(\alpha_T > 0.55)$ vs H_T in SM simulation. In all cases, $F(\alpha_T > 0.55)$ is consistent with having no H_T dependence.

is designed specifically to reject QCD events with artificial $\not{H}_T$ due to below-threshold jets, is removed. This causes $F(\alpha_T > 0.55)$ to be a decreasing function of H_T, indicating that there is a significant QCD background (i.e. artificial $\not{H}_T$) contribution.

In data, $F(\alpha_T > 0.55)$ is consistent with having no H_T dependence, which indicates that the $t\bar{t}$ and EWK backgrounds dominate. The larger anti-tagged data sample is also consistent with having no H_T dependence. Because a tight b-tag requirement only further suppresses the QCD background, the tight tagged sample is expected to have a negligible QCD contribution.

We perform a simple extrapolation of $F(\alpha_T > 0.55)$ from a lower H_T, 250-350 GeV, control region to the final signal region. To estimate the total background, $F(\alpha_T > 0.55)$ is measured in this control region and multiplied by the number of events in the signal region before the $\alpha_T >$

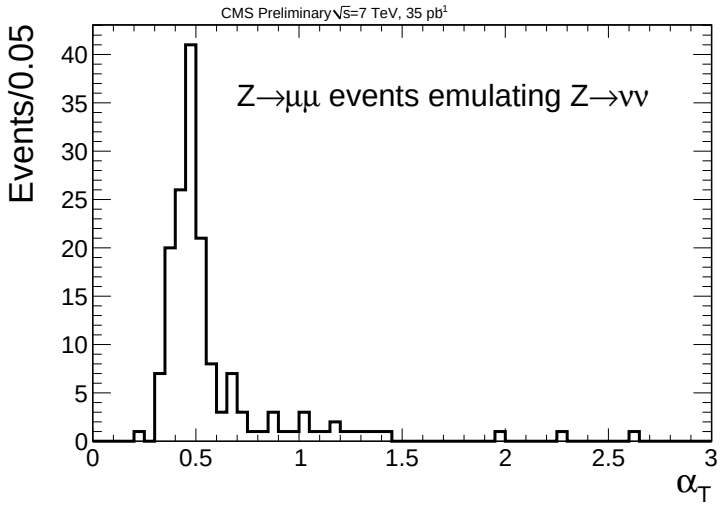

Figure 3: The α_T distribution for a $Z \to \mu^+\mu^-$ + jets sample. To mimic $Z \to \nu\bar{\nu}$ events, the muons are not included in the α_T calculation, which causes a significant tail beyond $\alpha_T > 0.55$.

0.55 requirement.

Applying this procedure to the data yields $F(\alpha_T > 0.55) = 1.48^{+1.93}_{-1.48} \times 10^{-5}$ and a prediction of $0.33^{+0.43}_{-0.33}$ (stat) events. The statistical uncertainty on this prediction is determined by the presence of one event with $\alpha_T > 0.55$ in the control sample.

If we require instead a loose b-tag in the control sample, we find $F(\alpha_T > 0.55) = 2.04 \pm 0.59 \times 10^{-5}$. The difference in $F(\alpha_T > 0.55)$ measured in the tight and loose tagged samples is taken as a systematic uncertainty on the prediction. Therefore, the final background estimate in this analysis is $0.33^{+0.43}_{-0.33}$ (stat) $\pm$ 0.13 (syst) events.

5.2 Cross Checks with $Z \to \nu\bar{\nu}$ and $t\bar{t}$ Events

It is useful, especially in case of an excess observation in data, to obtain a cross check on the $Z \to \nu\bar{\nu}$ background, which is expected to be the dominant EWK background contribution.

To estimate $Z \to \nu\bar{\nu}$, a sample of $Z \to \mu^+\mu^-$ events is selected with two or more jets and no other kinematic requirements and the fraction of events containing a b-tagged jet is measured. Figure 3 shows the resulting α_T distribution. Then, a sample is selected with no b-tag requirement, jet $E_T > 75$ GeV thresholds on the two leading jets, $H_T > 275$ GeV, and $\alpha_T > 0.52$. Note that these requirements are slightly looser than the final signal selection. The number of events in this sample is scaled by the measured b-tag fraction, corrected for the muon identification efficiency and acceptance, and multiplied by $\frac{BR(Z \to \nu\bar{\nu})}{BR(Z \to \mu^+\mu^-)} \approx 6$. This procedure gives an over-prediction of the number of $Z \to \nu\bar{\nu}$ events in the signal region due to less stringent requirements than the final selection, and yields 0.48 ± 0.39 events, which is consistent with the prediction from Section 5.1.

The muon selection criteria for the above $Z \to \mu^+\mu^-$ sample are loosened from those used in the lepton veto in order to increase selection efficiency. In particular, we loosen the requirements on the muon candidate track as measured by the tracker. We select events with exactly two muons with dimuon invariant mass near that of the Z boson ([81,101] GeV). Non Z contamination is predicted using events in the sideband mass regions [71-81] and [101,111] GeV. The resulting muon identification efficiency times acceptance is taken from simulation as 96%.

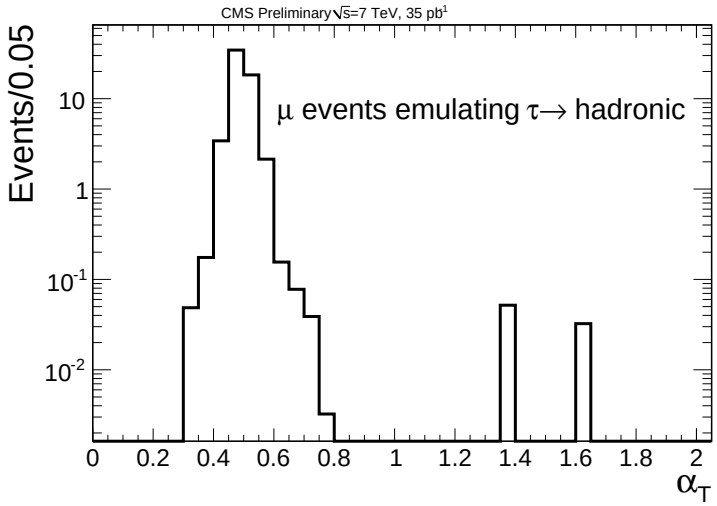

Figure 4: The α_T distribution for a $t\bar{t}$ dominated sample in which muons are used to emulate hadronic tau decays. The tail beyond $\alpha_T > 0.55$ results from the momentum imbalance due to emulated tau decays.

The number of $Z \to \mu^+\mu^-$ events measured in data agrees with simulation predictions within the 15% measurement uncertainty, which is taken as the uncertainty on the simulation based efficiency determination.

5.3 $t\bar{t}$ Cross Check

Because $t\bar{t}$ is expected to be the dominant background, it is important to estimate its contribution using more than one method. Simulation studies indicate that most, 72%, of the $t\bar{t}$ background comes from events with hadronic tau decays. The remainder is comprised of events with electrons and muons (15%), and events in which both W bosons decay hadronically (13%).

To estimate the hadronic tau decay yield, events are selected with one or two muons, used to emulate the hadronic decays of taus. For each muon, the presence of a jet is emulated with E_T taken as some fraction, with distribution taken from simulation, of the muon p_T. A less stringent version of the final event selection is used in which the E_T threshold of the leading two jets is 80 GeV, the H_T requirement is 280 GeV, and a medium b-tag is required. Figure 4 shows the resulting α_T distribution. The measured value of $F(\alpha_T > 0.55)$ in this sample is multiplied by the total number of emulated events in the signal region with no α_T requirement. This value is corrected for the muon selection efficiency and acceptance and the hadronic tau decay branching ratio to obtain the hadronic tau decay yield. To account for the entire $t\bar{t}$ background, the predicted hadronic tau decay yield is scaled by a simulation derived factor. We assign a 50% systematic error on this scaling, which is dominated by the statistical error on the prediction.

This procedure yields a slight over prediction in $t\bar{t}$ simulation. Applying the procedure in data predicts 1.41 ± 0.51 events. Note that these estimates are made for the three or more jet case only; the $t\bar{t}$ contribution to the two jet case is negligible, e.g., in simulation it is 0.01 times the three or more jet contribution.

This cross check of the $t\bar{t}$ background as well as that of $Z \to \nu\bar{\nu}$ in Section 5.2 confirm that the total background is small and consistent with the inclusive prediction, as would be crucial if there had been an observed excess.

Table 1: Background predictions with errors from SM simulation, scaled to 35 pb^{-1}.

N-jets	QCD	$t\bar{t}$	W	$Z \to \nu\bar{\nu}$	$Z \to l^+l^-$	total
2	0 ± 0.11	0.01 ± 0.01	0 ± 0.1	0 ± 0.09	0 ± 0.09	0.01 ± 0.21
≥ 3	0.05 ± 0.05	1.08 ± 0.07	0.10 ± 0.10	0.38 ± 0.18	0 ± 0.09	1.61 ± 0.26

Table 2: Predicted and observed events for 35 pb^{-1}. The prediction comes from the α_T vs H_T extrapolation described in Section 5.1. The LM0 uncertainty is statistical only.

N-jets	MC	Background Prediction	Data	LM0
≥ 2	1.61 ± 0.26	$0.33^{+0.43}_{-0.33}$ (stat) ± 0.13 (syst)	1	14.2 ± 0.3

5.4 Background Summary

For purely comparison purposes, Tab. 1 lists the SM simulation predictions for each background normalized to 35 pb^{-1}. Table 2 lists this prediction along with the observation in data, which is consistent, and the expected contribution of SUSY signal point LM0.

To confirm that this analysis responds to a real signal, a test is performed in which the isolated muon veto is inverted and α_T is determined after excluding the muon(s). This test yields four observed events, which is consistent with the 2.4 events predicted by simulation.

6 Signal Selection Efficiency

To interpret the results of this search in terms of a given model, the selection efficiency for that model must be determined. Table 3 lists the cumulative and individual efficiencies for the event selection in three SUSY benchmark models LM0, LM1, and LMB, from which events are generated via PYTHIA 6.4, tune Z2 [21]. Without b tagging, the cumulative efficiencies for LM0 and LM1 are about 85% of those in Ref. [11], due to a stricter lepton and photon veto.

7 Systematic Uncertainty on the Signal Selection Efficiency

Table 4 lists the systematic uncertainties on the signal selection efficiency, which are dominated by the uncertainty on the b-tagging efficiency, described in Sec 7.1. The other uncertainties and the methods used to obtain them are similar to those of Ref. [11], and are described briefly below.

Luminosity: The uncertainty on the luminosity is 11% [22].

Jet Energy Scale (JES): The JES is varied by $\pm 5\%$ [23]. This changes the average signal yield in a number of CMSSM model points by roughly 3.5%, which is taken as the systematic error due to JES uncertainty.

Jet Energy Resolution: The energy resolution of jets in simulation is better than in the data by 10 to 15% with some dependence on jet E_T and $|\eta|$. Jets are smeared to match the resolution in data and the resulting average signal yield changes by less than 1%, which we take as the systematic uncertainty for the effects of jet energy resolution.

Trigger Efficiency: The fraction of data events passing a lower threshold trigger that also pass

Table 3: Cumulative and individual efficiencies for the selection in three SUSY benchmark models LM0, LM1, and LMB. The total number of LM0, LM1, and LMB events before any selection are 219595, 219190, and 90000 respectively. For each model, the left and right columns represent the cumulative and individual efficiencies, respectively. Different models have different b-tag efficiencies due to different average numbers of b quarks per event. The fraction of events containing at least one b quark is only shown for illustration.

	LM0		LM1		LMB	
Requirement					Cumulative	Individual
Pre-selection	98%	98%	98%	98%	98%	98%
Lepton/Photon Veto	56%	57%	54%	55%	60%	61%
Jet Requirements	28%	51%	34%	63%	33%	54%
$H_{\mathrm{T}} > 350$ GeV	25%	90%	32%	94%	32%	97%
Trigger	25%	99%	32%	99%	31%	99%
Inactive ECAL cleaning	21%	82%	28%	88%	25%	80%
$\not{H}_{\mathrm{T}}/\not{E}_{\mathrm{T}} < 1.25$	17%	81%	26%	94%	20%	80%
≥ 1 b quark		66%		18%		91%
Tight b-tag	5.3%	31%	3.0%	12%	11%	54%
$\alpha_{\mathrm{T}} > 0.55$	0.7%	14%	0.9%	29%	1.3%	12%

Table 4: Systematic uncertainties on the signal selection efficiency.

Source	Uncertainty (%)
Luminosity	11%
JES	3.5%
Jet Energy Resolution	1%
Trigger Efficiency	1%
$\not{H}_{\mathrm{T}}/\not{E}_{\mathrm{T}} < 1.25$	2%
Inactive ECAL cleanup	3%
Lepton/Photon Veto	4%
b-tag Efficiency	20%
Total	24%

the trigger in the final selection is measured. A trigger efficiency of $99.37 \pm 0.07\%$ is determined.

$\not{H}_{\mathrm{T}}/\not{E}_{\mathrm{T}}$: This requirement rejects less than 4% of signal events, on average. Since this is such a small rejection, we take half, 2%, as the signal uncertainty due to this requirement.

Inactive ECAL cleanup: One source of uncertainty for the signal selection efficiency of this requirement comes from the variation of event topologies and kinematics in SUSY parameter space. This is estimated from the variation of the efficiencies in a few signal model points as roughly 2%. An additional contribution to the uncertainty is the ΔR resolution of jets [24]. Varying the ΔR of jets by their resolution gives a 2.2% uncertainty on the efficiency. An overall signal uncertainty due to this requirement is taken to be 3%.

Lepton/Photon Veto: The lepton/photon veto can be separated into two components, namely vetoes due to leptons and photons that are "good" or "odd". Good leptons and photons pass both identification and isolation requirements. Odd electrons and photons do not overlap a jet. An odd muon either does not overlap a jet or is a poor quality muon candidate. Taking a

conservative 10% uncertainty on the good lepton and photon identification efficiency [17–19, 25], a 2.3% systematic uncertainty on the signal efficiency due to the good lepton/photon veto is obtained. To study the odd lepton/photon veto, we select a QCD background dominated data sample and compare the efficiency of the veto to that of a QCD MC sample. The odd lepton/photon veto is found to reject more events in the data. After reducing the efficiency in simulation to correct for this difference, a variation of 3.3% is seen in the odd lepton/photon veto efficiency in a number of signal sample points. Combining the results for the good and odd lepton and photon vetoes gives a 4% systematic uncertainty on the signal efficiency and a 5% overall reduction in signal selection efficiency.

7.1 Systematic Uncertainty on the b-tagging Efficiency

The dominant uncertainty on the signal selection efficiency comes from limited knowledge of the b-tagging efficiency, ϵ_b, in data. The b-tagging efficiency is measured from inclusive di-jet events in which one jet has an associated muon and another "away" jet has a TCHP value of least 1.0. These two jets must be $\Delta R > 1.5$ away from one another. The relative fraction of jets from b quarks in a data sample is determined by a fit to the transverse momentum of muons relative to their associated jet axis, p_T^{rel} [10], which is larger for jets from b quarks than from other flavours. The measured p_T^{rel} distribution is fit to a linear combination of simulation derived p_T^{rel} templates from different flavours. The fit is restricted to the range $0 < p_T^{rel} < 3\,\text{GeV}$, in which the templates provide a reasonable description of the data.

The b-tagging efficiency is extracted from the fitted fraction of b quarks for jets passing and failing the analysis b-tagging requirement using

$$\epsilon_b = \frac{f_{\text{tagged}} \times N_{\text{tagged}}}{f_{\text{tagged}} \times N_{\text{tagged}} + f_{\text{untagged}} \times N_{\text{untagged}}} \tag{3}$$

where f_{tagged} and f_{untagged} are the respective fitted b fractions. This efficiency is measured separately for jets with $|\eta| > 1.4$ and $|\eta| < 1.4$, for four ranges of jet E_T. The ratio between the b-tagging efficiency measured in data and the estimate from simulation is taken as the efficiency scale factor for a particular range in E_T and $|\eta|$.

The resulting E_T and η dependent scale factors, with corresponding statistical uncertainties, are applied to signal MC. An overall selection efficiency of $(1.33 \pm 0.18)\%$ is found for the LMB benchmark point. The above relative uncertainty of 14% is taken as the average b-tagging statistical uncertainty. The statistical uncertainties found for the LM0 and LM1 benchmark points are 11% and 16%, respectively.

Systematic uncertainties on the scale factors arise from potential biases in the p_T^{rel} fitting procedure. These uncertainties are measured by varying the muon to jet matching and muon p_T thresholds, fraction of gluon splitting to $b\bar{b}$, jet energy scale and resolution, jet angular resolution, and b-tagging requirement on the away jet. The effect of measuring the scale factors using only semi-leptonic b decays is also accounted. These systematic uncertainties total 15% for the LMB signal point and together with the statistical uncertainty, yield a total uncertainty of 20%. The ratio of event yields in LMB with and without the scale factors applied is 0.87 ± 0.18.

8 Results

The observation of one data event in the signal region is consistent with background expectations. We illustrate the constraints that this measurement places on SUSY models by calculating cross section upper limits. The observation in data, estimated background from Section 5.1, and

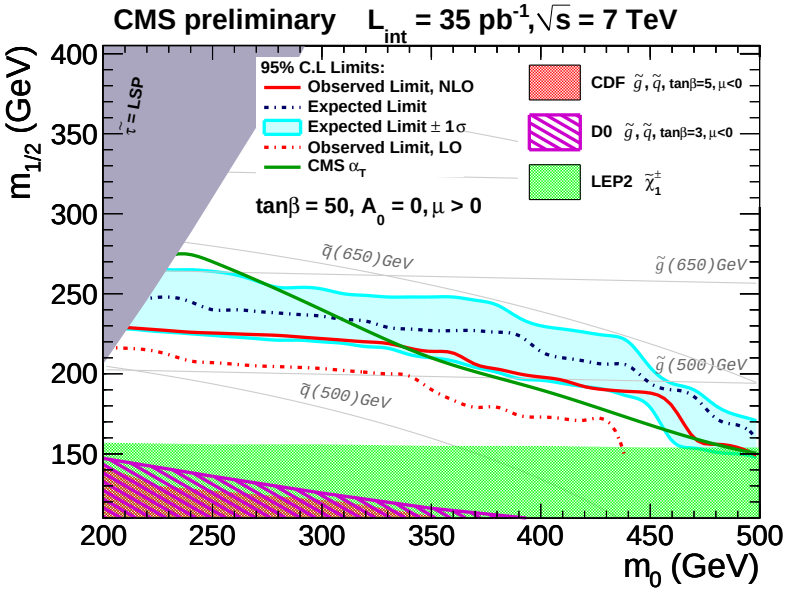

Figure 5: Exclusion regions in the ($m_{1/2}$, m_0) plane for one set of CMSSM parameters, for this analysis (red), and the non-b tagged version [11] (green).

24% systematic uncertainty on the signal selection efficiency, allow the determination of a 95% confidence level (C.L.) upper limit on the predicted number of observed signal events (N_{95}^{obs}). Using frequentist statistical methods in the manner of Ref. [26], with the use of the Profile Likelihood ratio [27] to handle nuisance parameters, it is found that $N_{95}^{\text{obs}} = 4.7$.

A 95% confidence level upper limit on the cross section (σ_{95}^{obs}) of a given model can be found using the equation

$$\sigma_{95}^{\text{obs}} = \frac{N_{95}^{\text{obs}}}{\mathcal{L} \cdot (\text{Efficiency})}, \tag{4}$$

where $\mathcal{L}$ denotes the luminosity and Efficiency denotes the signal selection efficiency. Using the signal selection efficiency values obtained in Section 6 for LM0, LM1, and LMB, we find σ_{95}^{obs} of 18.9, 15.4, and 10.2 pb, respectively. The possible over prediction of background due to signal contamination in the control regions increases σ_{95}^{obs} in LM0(LM1) to 22.1(16.7) pb but has a negligible effect in LMB. To quantify the sensitivity with reduced dependence on the amount of b quark production, a 95% C.L. upper limit on the cross section times branching ratio to at least one b quark, $\sigma_{95}^{\text{obs}} \cdot \text{BR}(\geq 1\text{b})$, of 4.0 pb is determined in LM1.

Figure 5 shows the excluded region in the ($m_{1/2}$, m_0) plane for CMSSM parameters $A_0 = 0$ GeV, $\tan\beta = 50$, and $\mu > 0$. The excluded region is extended with respect to that of Ref. [11] without b tagging, also shown, values of m_0 above 350 GeV, where b production is frequent. For models with infrequent b production, Ref. [11] sets more stringent limits, whereas this analysis has greater sensitivity to models with frequent b production.

9 Conclusion

A search for events with multiple jets, at least one of which must be b tagged, and significant transverse momentum imbalance has been presented. The dominant background comes from $\text{t}\bar{\text{t}}$. One event is observed, consistent with expectation. The results of the search are characterized as an exclusion region in SUSY parameter space and 95% C.L. upper limits of 18.9, 15.4, and 10.2 pb on the cross sections of LM0, LM1 and LMB, respectively.

References

[1] J. Wess and B. Zumino, "Supergauge Transformations in Four Dimensions", *Nucl. Phys.* **B 70** (1974) 39. doi:10.1016/0550-3213(74)90355-1.

[2] H. P. Nilles, "Supersymmetry, Supergravity and Particle Physics", *Phys. Reports* **110** (1984) 1. doi:10.1016/0370-1573(84)90008-5.

[3] H. E. Haber and G. L. Kane, "The Search for Supersymmetry: Probing Physics Beyond the Standard Model", *Phys. Reports* **117** (1987) 75. doi:10.1016/0370-1573(85)90051-1.

[4] R. Barbieri, S. Ferrara, and C. A. Savoy, "Gauge Models with Spontaneously Broken Local Supersymmetry", *Phys. Lett.* **B 119** (1982) 343. doi:10.1016/0370-2693(82)90685-2.

[5] S. Dawson, E. Eichten, and C. Quigg, "Search for Supersymmetric Particles in Hadron-Hadron Collisions", *Phys. Rev.* **D 31** (1985) 1581. doi:10.1103/PhysRevD.31.1581.

[6] E. Witten, "Dynamical Breaking of Supersymmetry", *Nucl. Phys.* **B 188** (1981) 513. doi:10.1016/0550-3213(81)90006-7.

[7] S. Dimopoulos and H. Georgi, "Softly Broken Supersymetry and SU(5)", *Nucl. Phys.* **B 193** (1981) 150. doi:10.1016/0550-3213(81)90522-8.

[8] G. Jungman and M. Kamionkowski, "Supersymmetric Dark Matter", *Phys. Rept.* **267** (1996) 195. doi:10.1016/0370-1573(95)00058-5.

[9] L. Randall and D. Tucker-Smith, "Dijet Searches for Supersymmetry at the LHC", *Phys.Rev.Lett.* **101** (2008) 221803. doi:10.1103/PhysRevLett.101.221803.

[10] CMS Collaboration, "Commissioning of b-jet identification with pp collisions at $\sqrt{s} = 7$ TeV", *CMS Physics Analysis Summary* **BTV-10-001** (2010).

[11] CMS Collaboration, "Search for supersymmetry in pp collisions at 7 TeV in events with jets and missing transverse energy", *Phys. Lett.* **B 698** (2011) 196. doi:10.1016/j.physletb.2011.03.021.

[12] G. L. Kane, C. Kolda, L. Roszkowski et al., "Study of Constrained Minimal Supersymmetry", *Phys. Rev.* **D 49** (1994) 6173. doi:10.1103/PhysRevD.49.6173.

[13] CMS Collaboration, "The CMS experiment at the CERN LHC", *JINST* **0803** (2008) S08004. doi:10.1088/1748-0221/3/08/S08004.

[14] CMS Collaboration, "Tracking and Primary Vertex Results in First 7 TeV Collisions", *CMS Physics Analysis Summary* **TRK-10-005** (2010).

[15] M. Cacciari, G. P. Salam, and G. Soyez, "The anti-kt jet clustering algorithm", *JHEP* **0804:063** (2008). doi:10.1088/1126-6708/2008/04/063.

[16] CMS Collaboration, "Calorimeter Jet Quality Criteria for the First CMS Collision Data", *CMS Physics Analysis Summary* **JME-09-008** (2009).

[17] CMS Collaboration, "Isolated Photon Reconstruction and Identification at $\sqrt{s} = 7$ TeV", *CMS Physics Analysis Summary* **EGM-10-006** (2010).

[18] CMS Collaboration, "Electron reconstruction and identification at $\sqrt{s}$ = 7 TeV", *CMS Physics Analysis Summary* **EGM-10-004** (2010).

[19] CMS Collaboration, "Performance of muon identification in pp collisions at $\sqrt{s}$ = 7 TeV", *CMS Physics Analysis Summary* **MUO-10-002** (2010).

[20] J. Alwall et al., "MadGraph/MadEvent v4: The New Web Generation", *JHEP* **09** (2007) 028. doi:10.1088/1126-6708/2007/09/028.

[21] T. Sjöstrand, S. Mrenna, and P. Skands, "PYTHIA 6.4 Physics and Manua", *JHEP* **05** (2006) 026. doi:10.1088/1126-6708/2006/05/026.

[22] CMS Collaboration, "Measurement of CMS luminosity", *CMS Physics Analysis Summary* **EWK-10-004** (2010).

[23] CMS Collaboration, "Jet Energy Corrections determination at 7 TeV", *CMS Physics Analysis Summary* **JME-10-010** (2010).

[24] CMS Collaboration, "Jet Performance in pp Collisions at $\sqrt{s} = 7$ TeV", *CMS Physics Analysis Summary* **JME-10-003** (2010).

[25] CMS Collaboration, "Measurements of Inclusive W and Z Cross Sections in pp Collisions at $\sqrt{s} = 7$ TeV with the CMS experiment at the LHC", *CMS Physics Analysis Summary* **EWK-10-002** (2010).

[26] G. J. Feldman and R. D. Cousins, "A Unified Approach to the Classical Statistical Analysis of Small Signals", *Phys. Rev.* **D57** (1998) 3873. doi:10.1103/PhysRevD.57.3873.

[27] T. A. Severini, "Likelihood Methods in Statistics". Oxford University Press, 2000.

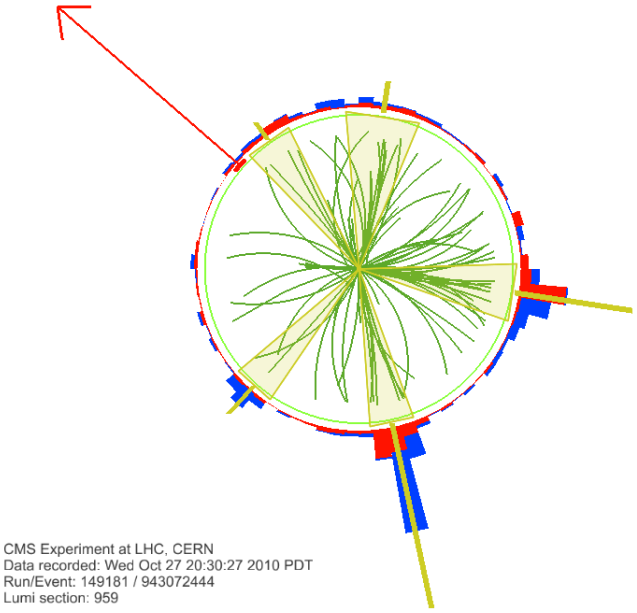

Figure 6: A display of the one data event in the signal region projected onto the transverse plane. The yellow triangles correspond to jets with $E_{\mathrm{T}} > 50$ GeV. The red arrow corresponds to the $\not\!\!E_{\mathrm{T}}$.

A Data Event in Signal Region

As shown in Tab. 2, one event was observed in the signal region, namely run= 149181, event= 943072444, and was also observed in [11]. This event has four jets with $E_{\mathrm{T}} > 50$ GeV. One of these jets passes the tight b-tag requirement with discriminator value $TCHP = 13.6$. There are no muons and one non-isolated electron and photon that each coincide with a jet. Relevant kinematic values for this event are $H_{\mathrm{T}} = 457$ GeV, $\not\!\!H_{\mathrm{T}} = 263$ GeV, $\phi(\not\!\!H_{\mathrm{T}}) = 2.20$ rad, $\not\!\!E_{\mathrm{T}} = 212$ GeV, $\phi(\not\!\!E_{\mathrm{T}}) = 2.35$ rad. The $\not\!\!H_{\mathrm{T}}$ and $\not\!\!E_{\mathrm{T}}$ are similar in both magnitude and direction. The event has $\alpha_{\mathrm{T}} = 0.5561$. Figure 6 is a display of this event in the transverse plane. The yellow triangles correspond to jets, and the red arrow corresponds to the $\not\!\!E_{\mathrm{T}}$.